



Unified Personalized Reward Model for Vision Generation

Yibin Wang^{1,2}, Yuhang Zang^{4†}, Feng Han^{1,2},
Yujie Zhou^{3,4}, Jiazi Bu^{3,4}, Cheng Jin^{1,2†}, Jiaqi Wang^{2†}

¹Fudan University ²Shanghai Innovation Institute

³Shanghai Jiaotong University ⁴Shanghai AI Lab

Abstract

Recent advancements in multimodal reward models (RMs) have significantly propelled the development of visual generation. Existing frameworks typically adopt Bradley–Terry-style preference modeling or leverage generative vision-language models (VLMs) as judges, and subsequently optimize visual generation models via reinforcement learning. However, current RMs suffer from inherent limitations: they often follow a “one-size-fits-all” paradigm that assumes a monolithic preference distribution or relies on fixed evaluation rubrics. As a result, they are insensitive to content-specific visual cues, leading to systematic misalignment with subjective and context-dependent human preferences. To this end, inspired by human assessment, we propose **UNIFIEDREWARD-FLEX**, a unified personalized reward model for vision generation that couples reward modeling with flexible and context-adaptive reasoning. Specifically, given a prompt and the generated visual content, it first interprets the semantic intent and grounds on visual evidence, then dynamically constructs a hierarchical assessment by instantiating fine-grained criteria under both predefined and self-generated high-level dimensions. Our training pipeline follows a two-stage process: (1) we first distill structured, high-quality reasoning traces from advanced closed-source VLMs to bootstrap supervised fine-tuning (SFT), equipping the model with flexible and context-adaptive reasoning behaviors; (2) we then perform direct preference optimization (DPO) on carefully curated preference pairs to further strengthen reasoning fidelity and discriminative alignment. To validate the effectiveness, we integrate **UNIFIEDREWARD-FLEX** into the Group Relative Policy Optimization (GRPO) framework for image and video synthesis. Extensive results demonstrate its superiority: it consistently delivers more robust, context-aware reward signals than existing baselines and achieves substantial improvements in both image and video synthesis.

Website: <https://codegoat24.github.io/UnifiedReward/flex>

1 Introduction

With the rapid progress of multimodal reward models (RMs) [1, 2, 3, 4, 5], their potential in aligning vision generation models with human preferences has attracted growing attention. By converting subjective and high-level human judgments into learnable reward signals, RMs enable effective preference-driven post-training for vision generators. [6, 7, 8, 9, 10, 11]. Early reward modeling for visual generation typically

[†]Corresponding authors.

uses fixed, discriminative scorers [12, 13, 14, 15] to assign scalar rewards. Later works shift to Bradley–Terry [16] pairwise preference modeling to learn rewards from relative comparisons [4, 17]. More recently, VLM-as-a-judge [1, 2, 3, 18] has emerged, leveraging strong generative VLMs [19, 20] to provide context-dependent evaluations for reinforcement learning.

Despite their effectiveness, current RMs often follow a “one-size-fits-all” assessment paradigm: (1) Fixed discriminative scorers (e.g., CLIP [12], PickScore [15]) and Bradley–Terry preference models (e.g., VideoAlign [4], HPSv3 [17]) typically learn a single global reward function that assigns a scalar score to each input (or induces preferences via score differences), implicitly assuming a monolithic preference distribution shared across diverse prompts and visual contents. (2) VLM-as-a-judge approaches (e.g., UnifiedReward-Think [2]) leverage generative VLMs to produce richer textual judgments, yet they often follow static evaluation rubrics with a fixed checklist of criteria. As a result, their reward feedback remains insensitive to content-specific visual cues, which can misguide optimization and cause systematic misalignment with human preferences.

In this work, we posit that reliable reward assessment should be flexibly adapted to the prompt intent and visual content. For example, prompts with implicit narrative intent should emphasize storytelling consistency, subject relationships, and emotional tone (see Fig. 1), whereas motion-intensive videos with frequent physical contact demand explicit evaluation of action dynamics and physical plausibility (see Fig. 2). This behavior closely mirrors how humans assess visual generations: evaluators first interpret the prompt intent and the depicted content, then evaluate along a small set of common, task-specific high-level dimensions. Within each dimension, they selectively attend to the aspects most relevant to the given instance. When the scene exhibits additional characteristics, evaluators naturally introduce new high-level dimensions to capture these salient factors. In other words, human evaluation is inherently a content-adaptive, context-aware reasoning process, where both the evaluation criteria and their relative importance are dynamically adjusted to match the semantic intent and visual evidence.

As inspired, this work proposes **UNIFIEDREWARD-FLEX**, a unified personalized reward model for vision generation that couples reward modeling with context-adaptive reasoning to dynamically tailor evaluation criteria, which performs assessment in a hierarchical manner. Specifically, given a prompt and the generated visual content, it first interprets the semantic intent and extracts salient visual evidence, then composes a hierarchical evaluation plan by instantiating fine-grained sub-criteria under a few predefined coarse-grained dimensions. When the context demands additional considerations, it augments the hierarchy with new high-level dimensions and their corresponding sub-criteria. This dynamic criterion composition yields adaptive and informative reward feedback that aligns with the human evaluation process and remains robust across diverse prompts and visual content. Our training follows a two-stage pipeline: (1) We first distill structured, high-quality reasoning traces from advanced closed-source VLMs [21] to bootstrap supervised fine-tuning (SFT), endowing the model with content-aware criterion composition. (2) We then apply direct preference optimization (DPO) using preference pairs with human-grounded labels: given two sampled responses for the same input, if one reaches the correct conclusion while the other does not, the preference naturally favors the correct one; if both are correct, we further assign the preference based on the quality of their adaptive reasoning trajectories, prioritizing more flexible and context-grounded evaluation hierarchies. Empirically, this reasoning-aware preference alignment improves the reward model’s discriminative power, even among samples that are all correct.

Extensive experiments show that **UNIFIEDREWARD-FLEX** consistently outperforms strong reward model baselines on both image and video reward tasks, providing more robust and context-aware reward signals. To further validate its practical utility, we use it as the reward signal for pairwise preference reward-based GRPO [6] in both image and video synthesis, yielding substantial quantitative and qualitative improvements in downstream generation quality.

Contributions. (1) We identify a key limitation of existing multimodal reward models, i.e., their “one-size-fits-all” evaluation paradigm, and propose **UNIFIEDREWARD-FLEX**, a unified personalized reward model for vision generation that dynamically composes evaluation hierarchies via content-aware reasoning. (2) Our **UNIFIEDREWARD-FLEX** consistently outperforms strong reward model baselines on both image and video reward tasks, delivering more robust and context-aware reward signals. (3) We further validate its practical utility by integrating it into pairwise preference reward-based GRPO for image and video synthesis, achieving substantial improvements in downstream generation quality both quantitatively and qualitatively.



Figure 1 Qualitative Result of UNIFIEDREWARD-FLEX on Image Generation Personalized Reward Reasoning.

2 Related Work

Multimodal Reward Models (RMs) are crucial in aligning vision generation models with human preferences. Early reward modeling typically relies on **fixed, discriminative scorers** that assign a scalar score to each generated sample [12, 13, 14, 15]. These scorers are lightweight and easy to deploy, but they often behave as task-agnostic heuristics: the reward function is largely fixed across prompts and contents, making it difficult to reflect diverse evaluation focuses. To better capture the relative nature of human judgment, later works shift from absolute scoring to pairwise preference modeling under the **Bradley-Terry pairwise preference modeling** [16]. Instead of regressing a single target score, the RM is trained to assign higher reward to preferred samples within a comparison pair, which often yields more stable and better calibrated training signals for preference optimization [4, 5, 17]. Nevertheless, Bradley-Terry based RMs still typically learn a single global scalar reward function shared across heterogeneous prompts and visual contents, implicitly assuming a monolithic preference distribution. More recently, **VLM-as-a-judge** has emerged as a flexible alternative that leverages strong generative VLMs to directly assess and compare candidates [1, 2, 3, 18, 22]. Compared to discriminative scorers, these judge models can provide richer evaluative feedback, potentially incorporating multi-aspect reasoning and content-dependent judgments. However, existing VLM-judge approaches commonly follow static evaluation rubrics or fixed checklists of criteria, which limits their ability to dynamically tailor evaluation priorities to the semantic intent and visual evidence of each input. To this end, this work proposes **UNIFIEDREWARD-FLEX**, a unified personalized reward model for vision generation that couples reward modeling with content-aware reasoning. Unlike prior RMs that apply a fixed global scoring function or static rubrics, UNIFIEDREWARD-FLEX dynamically constructs a context-adaptive hierarchical



Figure 2 Qualitative Result of UNIFIEDREWARD-FLEX on Video Generation Personalized Reward Reasoning.

assessment by self-instantiating fine-grained criteria based on given prompt intent and visual evidence. *Reinforcement Learning for Vision Generation* has evolved rapidly in recent years. Early attempts either fine-tuned models with scalar reward supervision [23, 24] or adopted reward-weighted regression to exploit reward feedback in a more stable manner [3, 4, 25]. Subsequent work drew inspiration from Proximal Policy Optimization (PPO) [26] and incorporated policy-gradient updates into diffusion-based generators, showing promising improvements in sample quality [27, 28, 29]. Despite their effectiveness, these methods are often computationally demanding and sensitive to hyperparameter tuning. To improve training efficiency, a growing line of research explores preference optimization with supervised objectives, such as direct preference optimization (DPO), which directly leverages human preference data and avoids expensive on-policy rollouts [30, 31, 32, 33]. More recently, Group Relative Policy Optimization (GPRO) [34] has emerged as a promising objective for preference optimization in complex reasoning tasks. [9, 10] extend GRPO to flow matching models by reformulating the ODE sampling process as an equivalent SDE, enabling diverse sampling while performing preference-driven optimization. [7, 11, 35] further improve efficiency with a sliding-window mechanism that localizes SDE sampling and GRPO updates within a window while retaining ODE sampling elsewhere. However, these approaches typically optimize pointwise scalar rewards and may suffer from reward hacking [8, 9]. Pref-GRPO [6] reveals that reward hacking is largely driven by "illusory advantages" induced by unreliable reward signals, and stabilizes learning by replacing pointwise rewards with pairwise preference-based feedback. In this work, we integrate our UNIFIEDREWARD-FLEX into the Pref-GRPO framework for both image and video synthesis to validate its effectiveness.

3 Method

3.1 Overview

Multimodal reward models (RMs) serve as learned proxies for human visual preferences. However, existing RMs often follow a “one-size-fits-all” paradigm: they either assume a monolithic preference distribution captured by a single global scoring function, or rely on fixed evaluation rubrics that apply the same criteria uniformly across inputs. As a result, their reward feedback is often insensitive to content-specific visual cues and prompt intent, leading to systematic misalignment with inherently subjective and context-dependent human preferences. To this end, we propose **UNIFIEDREWARD-FLEX**, a unified personalized reward model for vision generation that couples reward modeling with context-adaptive reasoning to dynamically tailor evaluation criteria.

In this section, we first present our unified personalized reward modeling framework (Sec. 3.2), including the design of our context-adaptive reasoning process (Sec. 3.2.1) and a two-stage training pipeline: (i) reasoning distillation for SFT (Sec. 3.2.2) and (ii) reasoning-aware preference alignment via DPO (Sec. 3.2.3). We then describe how to apply **UNIFIEDREWARD-FLEX** to reinforcement learning for vision generation (Sec. 3.3), starting with the necessary preliminaries (Sec. 3.3.1), and followed by our employed personalized multi-dimensional preference rewards for GRPO (Sec. 3.3.2).

3.2 Unified Personalized Reward Modeling

3.2.1 Context-adaptive Reasoning Process Design

Our goal is to mimic how humans evaluate generated visual content. In practice, for a given task, human evaluators typically assess outputs along a small set of common high-level dimensions (e.g., semantic alignment and perceptual quality), while instantiating more fine-grained factors depending on the prompt intent and the visual evidence under each dimensions. When additional considerations become salient (e.g., Narrative & Interaction in Fig. 1), they naturally extend the evaluation dimensions to better capture what matters for the current instance.

Guided by this principle, we design a context-adaptive hierarchical reasoning process that starts from three predefined common dimensions as stable anchors (e.g., semantic alignment, visual quality, and aesthetics for image generation). Under each anchor, the model instantiates prompt-specific sub-dimensions for assessment, and it can further introduce new high-level dimensions (with corresponding sub-dimensions) when required by the context. For each high-level dimension, the model aggregates the evidence across its instantiated sub-dimensions to produce an overall comparative analysis and a dimension-level winner; it then combines the outcomes from all high-level dimensions to determine a final overall winner.

Specifically, as shown in Fig. 2, **UNIFIEDREWARD-FLEX** derives prompt-relevant sub-dimensions under the given anchors to jointly assess semantic adherence, visual quality under motion, and cinematographic coherence of generated videos. Since this case emphasizes rich motion and physical interactions, the model further introduces an additional high-level dimension (i.e., Action Dynamics & Physics) to explicitly evaluate temporal coherence and physical plausibility, which is then incorporated into the final overall decision.

By tailoring the evaluation hierarchy to the generation context, our model provides richer reward supervision for preference optimization, improving both intent satisfaction and content-critical quality factors.

3.2.2 Stage I: Reasoning Distillation for SFT

To bootstrap the model with context-adaptive assessment behaviors, we first distill structured reasoning traces from the powerful closed-source VLM [21] and use them for supervised fine-tuning (SFT).

Distillation data. Let $\mathcal{D} = \{x_i\}_{i=1}^N$ be a set of preference-evaluation instances, where each input

$$x_i = (p_i, v_i^{(0)}, v_i^{(1)}) \quad (1)$$

contains a text prompt p_i and a pair of candidate visual generations $(v_i^{(0)}, v_i^{(1)})$. Given x_i , the closed-source teacher model \mathcal{T} outputs a structured evaluation trace

$$y_i^{\mathcal{T}} = \mathcal{T}(x_i) = (\mathcal{H}_i, \mathcal{R}_i, \mathcal{W}_i), \quad (2)$$

where $\mathcal{H}_i = \{(d_k, \mathcal{S}_{i,k})\}_{k=1}^{K_i}$ denotes the instantiated high-level dimensions d_k together with their prompt-specific sub-dimensions $\mathcal{S}_{i,k}$, \mathcal{R}_i is the corresponding evidence-grounded reasoning trace, and $\mathcal{W}_i = (\{w_{i,k}\}_{k=1}^{K_i}, w_i)$ are winner labels. Here $w_{i,k} \in \{0, 1\}$ denotes the winner under dimension d_k and $w_i \in \{0, 1\}$ denotes the overall winner.

SFT objective. We fine-tune the base model [2] with parameters θ to imitate the teacher outputs via conditional language modeling:

$$\mathcal{L}_{\text{SFT}}(\theta) = -\sum_{i=1}^N \log p_\theta(y_i^{\mathcal{T}} | x_i) = -\sum_{i=1}^N \sum_{t=1}^{|y_i^{\mathcal{T}}|} \log p_\theta(y_{i,t}^{\mathcal{T}} | x_i, y_{i,<t}^{\mathcal{T}}). \quad (3)$$

This stage initializes the model to generate structured, context-adaptive evaluations for paired visual comparisons, providing a strong foundation for subsequent preference alignment.

3.2.3 Stage II: Reasoning-Aware Preference Alignment via DPO

Building on the SFT-initialized context-adaptive evaluations, we further optimize it for preference discrimination under human-grounded supervision. Specifically, we apply Direct Preference Optimization (DPO) to jointly align the final decision and the quality of the adaptive reasoning trajectory.

Preference pair construction. For each input $x_i = (p_i, v_i^{(0)}, v_i^{(1)})$, we assume an annotated preference label $w_i^* \in \{0, 1\}$ provided by the dataset, where $w_i^* = 0$ indicates $v_i^{(0)}$ is preferred and $w_i^* = 1$ indicates $v_i^{(1)}$ is preferred. Starting from the SFT model, we sample two candidate structured evaluations

$$y_i^{(a)}, y_i^{(b)} \sim \pi_\theta(\cdot | x_i), \quad (4)$$

each containing an overall predicted winner $\hat{w}(y) \in \{0, 1\}$ and a context-adaptive reasoning trace. We define the correctness indicator

$$c(y_i^{(j)}) = \mathbb{I}[\hat{w}(y_i^{(j)}) = w_i^*], \quad j \in \{a, b\}. \quad (5)$$

If exactly one sample is correct, we set the preference to favor the correct one. If both samples are correct, we further rank them by the quality of their adaptive reasoning trajectories, preferring evaluations with more context-grounded and flexible hierarchies. Concretely, when both samples are correct, we obtain a trajectory-level preference by querying a closed-source judge $\mathcal{T}_{\text{judge}}$ to perform pairwise comparison and output the preferred reasoning trace, followed by human verification on the judged pairs. We denote the judged preference as

$$\ell_i^{\text{traj}} = \mathcal{T}_{\text{judge}}(x_i, y_i^{(a)}, y_i^{(b)}) \in \{a, b\}, \quad (6)$$

where ℓ_i^{traj} indicates which trace is preferred in terms of reasoning quality. We then construct the DPO pair (y_i^+, y_i^-) as

$$(y_i^+, y_i^-) = \begin{cases} (y_i^{(a)}, y_i^{(b)}), & c(y_i^{(a)}) > c(y_i^{(b)}) \\ (y_i^{(b)}, y_i^{(a)}), & c(y_i^{(b)}) > c(y_i^{(a)}) \\ (y_i^{(\ell_i^{\text{traj}})}, y_i^{(\bar{\ell}_i^{\text{traj}})}), & c(y_i^{(a)}) = c(y_i^{(b)}) = 1, \end{cases} \quad (7)$$

where $\bar{\ell}_i^{\text{traj}} \in \{a, b\} \setminus \{\ell_i^{\text{traj}}\}$, and we discard the pair if $c(y_i^{(a)}) = c(y_i^{(b)}) = 0$. This construction aligns not only the final preference decision but also the quality of the underlying context-adaptive reasoning trajectory.

DPO objective. Given the resulting preference dataset $\mathcal{P} = \{(x_i, y_i^+, y_i^-)\}$, we optimize π_θ with the standard DPO loss using a frozen reference policy π_{ref} (the SFT model):

$$\mathcal{L}_{\text{DPO}}(\theta) = -\mathbb{E}_{(x, y^+, y^-) \sim \mathcal{P}} \left[\log \sigma(\beta_{\text{dpo}} (\log \pi_\theta(y^+ | x) - \log \pi_\theta(y^- | x) - \log \pi_{\text{ref}}(y^+ | x) + \log \pi_{\text{ref}}(y^- | x))) \right], \quad (8)$$

where β controls the strength of preference optimization. By directly increasing the likelihood of preferred structured evaluations, this stage sharpens the reward model's discriminative ability while reinforcing its

context-adaptive reasoning behavior. Empirically, such reasoning-aware preference alignment improves the reward model’s discriminative power, even among samples that are all correct.

3.3 Reinforcement Learning for Vision Generation

3.3.1 Preliminaries

Flow Matching GRPO. We briefly review GRPO [34] in the context of flow-matching models [9, 10]. Given a prompt c , a flow-based generator produces an image/video x_0 by iteratively refining a noisy sample from $t = T$ to $t = 0$. For each sample, we consider terminal reward supervision, where the reward is provided at the end of the trajectory as $R(x_0, c)$.

Group-relative advantage. Given a prompt c , GRPO samples a group of G generations $\{x_0^i\}_{i=1}^G$ and evaluates them with a reward model to obtain $\{R(x_0^i, c)\}_{i=1}^G$. To stabilize learning under noisy rewards, GRPO constructs a prompt-wise standardized advantage:

$$\hat{A}^i = \frac{R(x_0^i, c) - \mu_c}{\sigma_c}, \quad \mu_c = \text{mean}(\{R(x_0^j, c)\}_{j=1}^G), \quad \sigma_c = \text{std}(\{R(x_0^j, c)\}_{j=1}^G). \quad (9)$$

This relative advantage encourages the policy to increase the likelihood of higher-quality generations within the same prompt group, rather than chasing absolute reward values.

GRPO objective. Let π_θ denote the sampling policy induced by the generator, and $\pi_{\theta_{\text{old}}}$ be the behavior policy used to collect trajectories. For the i -th trajectory at step t , the importance ratio is

$$r_t^i(\theta) = \frac{\pi_\theta(x_{t-1}^i | x_t^i, c)}{\pi_{\theta_{\text{old}}}(x_{t-1}^i | x_t^i, c)}. \quad (10)$$

GRPO then maximizes a clipped surrogate objective with KL regularization to a reference policy π_{ref} :

$$\mathcal{J}_{\text{GRPO}}(\theta) = \mathbb{E}_c \left[\frac{1}{G} \sum_{i=1}^G \frac{1}{T} \sum_{t=0}^{T-1} \min \left(r_t^i(\theta) \hat{A}^i, \text{clip}(r_t^i(\theta), 1 - \eta, 1 + \eta) \hat{A}^i \right) - \beta_{\text{KL}} D_{\text{KL}}(\pi_\theta \| \pi_{\text{ref}}) \right], \quad (11)$$

where η is the clipping threshold and β_{KL} controls the strength of regularization. This formulation provides a principled and stable way to post-train vision generators with learned reward signals.

Pairwise Preference Reward-based GRPO (Pref-GRPO) [6] replaces absolute reward scores with relative preference judgments, which better align with the common practice of evaluating visual generations via pairwise comparisons. Instead of assigning an independent scalar reward to each sample, Pref-GRPO derives terminal rewards from comparative outcomes among a group of generated samples.

Given a prompt c , a group of G images (or videos) $\{x_0^i\}_{i=1}^G$ is sampled from the current policy π_θ . For each unordered pair (x_0^i, x_0^j) , a preference model determines which sample is preferred, denoted by $x_0^i > x_0^j$. Based on all pairwise comparisons within the group, Pref-GRPO defines a relative preference reward for each sample as its normalized win rate:

$$R(x_0^i, c) = \frac{1}{G-1} \sum_{j \neq i} \mathbb{1}(x_0^i > x_0^j), \quad (12)$$

which reflects how often sample i is preferred over other candidates under the same prompt.

These preference-derived rewards are then directly plugged into the standard GRPO framework. In particular, the group-relative advantage \hat{A}^i is computed using Eq. (9), and the policy is optimized with the same clipped surrogate objective in Eq. (11).

3.3.2 Personalized Multi-Dimensional Preference Rewards

In this work, we integrate our flexible, context-adaptive evaluations from `UNIFIEDREWARD-FLEX` into Pref-GRPO to provide personalized, multi-dimensional rewards. Specifically, given a prompt c , the policy π_θ

Table 1 Image and Video Generation Assessment Comparison.

Method	Image Generation		Method	Video Generation	
	GenAI-Bench	MMRB2		GenAI-Bench	MJ Bench
HPSv2	68.8	55.0	LiFT	60.1	51.0
PickScore	70.0	57.6	VideoScore	70.6	62.8
HPSv3	70.9	58.5	VideoReward	73.1	63.4
UnifiedReward	71.5	60.0	UnifiedReward	76.8	68.8
UnifiedReward-Think	<u>72.3</u>	66.0	UnifiedReward-Think	80.3	<u>70.9</u>
Ours w/o DPO	71.5	67.5	Ours w/o DPO	79.4	69.1
Ours w/o DPO (Both correct)	72.0	<u>68.4</u>	Ours w/o DPO (Both correct)	<u>80.6</u>	70.3
Ours	73.4	69.2	Ours	82.5	72.0

samples a group of G candidates $\{x_0^i\}_{i=1}^G$, and for each unordered pair (x_0^i, x_0^j) , the reward model produces pairwise preference judgments along D predefined anchor dimensions:

$$x_0^i \succ_d x_0^j, \quad d = 1, \dots, D.$$

For each candidate, we compute the dimension-wise win rates and their average over the anchor dimensions:

$$\bar{R}_{\text{dim}}(x_0^i, c) = \frac{1}{D} \sum_{d=1}^D R_d(x_0^i, c), \quad R_d(x_0^i, c) = \frac{1}{G-1} \sum_{j \neq i} \mathbb{1}(x_0^i \succ_d x_0^j).$$

To account for dynamic, personalized high-level dimensions that may not appear consistently in each pairwise comparison, we also compute the overall win rate:

$$R_{\text{overall}}(x_0^i, c) = \frac{1}{G-1} \sum_{j \neq i} \mathbb{1}(x_0^i \succ x_0^j).$$

The group-relative advantages are then computed separately for the averaged dimension-wise win rate and the overall win rate:

$$\hat{A}_{\text{dim}}^i = \frac{\bar{R}_{\text{dim}}(x_0^i, c) - \mu_{\text{dim}}}{\sigma_{\text{dim}}}, \quad \hat{A}_{\text{overall}}^i = \frac{R_{\text{overall}}(x_0^i, c) - \mu_{\text{overall}}}{\sigma_{\text{overall}}},$$

where μ and σ are the mean and standard deviation within the prompt group.

Finally, the combined advantage used in GRPO is

$$\hat{A}^i = \alpha \hat{A}_{\text{dim}}^i + (1 - \alpha) \hat{A}_{\text{overall}}^i,$$

where α controls the relative contributions of the averaged dimension-wise advantage and the overall advantage, respectively.

This procedure ensures that both the fine-grained anchor preferences and the holistic, context-adaptive evaluation contribute to the policy update, while remaining compatible with the training objective in Eq. (11).

4 Experiment

4.1 Implementation Details

4.1.1 UNIFIEDREWARD-FLEX

Datasets. For *image generation*, we sample 50K image preference pairs from HPDV3 [17]. For *video generation*, we combine two human preference datasets: Text2Video-Human Preferences (15K), provided by Rapidata, and VideoFeedback2 [18], from which we preprocess and construct an additional 35K video preference pairs. In the SFT stage, we distill reward reasoning traces for both images and videos from GPT-5.2 [21], using 45K image pairs and 45K video pairs to construct our *UnifiedReward-Flex-SFT-90K* dataset. Training samples are

Table 2 In-domain Semantic Consistency Comparison on UniGenBench. “UniGenBench-EvalModel-qwen3vl-32b-v1” is used as the VLM for evaluation.

Model	Overall	Style	World Know.	Attribute	Action	Relation.	Compound	Grammar	Logic.Reason.	Layout	Text
FLUX.1-dev	59.39	85.10	85.92	65.28	61.41	64.97	43.56	60.16	24.77	70.52	32.18
w/ HPSv2	57.77	77.90	87.03	65.92	57.41	65.86	44.46	55.75	29.09	64.93	29.31
w/ HPSv3	57.98	79.40	90.03	66.24	57.89	63.58	39.82	58.82	24.09	67.16	32.76
w/ PickScore	58.63	79.70	87.03	64.42	61.12	67.64	47.42	58.02	27.50	67.54	25.86
w/ UnifiedReward	60.87	83.50	87.97	66.13	63.88	68.65	46.52	58.69	24.32	71.08	37.93
w/ UnifiedReward-Think	68.89	88.00	91.77	<u>77.99</u>	69.20	75.13	<u>61.47</u>	<u>61.63</u>	<u>41.36</u>	<u>77.24</u>	<u>45.11</u>
w/ UnifiedReward-Flex	73.95	90.30	<u>89.87</u>	79.38	73.38	78.55	69.46	63.10	46.59	79.66	59.20

Table 3 Out-of-Domain Semantic Consistency and Image Quality Evaluations. The best results are in **bold**, and the second best are underlined.

Model	Semantic Consistency				Image Quality		
	UniGenBench	T2I-CompBench	GenEval	CLIP	PickScore	UnifiedReward	Aesthetic
FLUX.1-dev	59.39	48.57	62.18	34.40	22.70	3.07	6.13
w/ HPSv2	57.77	44.84	58.43	33.35	23.12	3.10	6.23
w/ HPSv3	57.98	46.46	61.14	34.12	23.26	3.14	6.37
w/ PickScore	58.63	45.92	58.76	33.61	23.78	3.12	6.42
w/ UnifiedReward	60.87	49.13	66.25	34.43	23.31	3.19	6.44
w/ UnifiedReward-Think	68.89	50.10	68.20	35.85	23.38	3.27	6.53
w/ UnifiedReward-Flex	73.95	51.37	69.62	36.25	<u>23.42</u>	<u>3.31</u>	<u>6.56</u>

randomly drawn from the collected datasets, while the remaining data are reserved for the subsequent DPO stage. In the DPO stage, we use non-greedy decoding with temperature 0.7 and sample two reasoning traces per prompt. If both samples yield the correct preference decision, we further use GPT-5.2 to perform pairwise comparison of their reasoning trajectories and select the higher-quality trace as the preferred response for constructing DPO training pairs.

Reward model. We adopt UnifiedReward-Think-qwen3vl-8B [2] as the base reward model, which supports long-chain reasoning for both visual perception and generation. Building on its strong prior knowledge, we further steer it toward flexible, context-adaptive reward reasoning.

Training details. Our training is conducted with a batch size of 2 and 2 gradient accumulation steps, using a learning rate of 2.5×10^{-6} and a warm-up ratio of 0.1. All experiments are performed on 32 NVIDIA H200 GPUs. For the DPO stage, we set β_{dpo} to 0.1.

Evaluation. We evaluate image reward models on GenAI-Bench-Image [36] and Multimodal RewardBench 2 (MMRB2) [37], and video reward models on GenAI-Bench-Video [36] and MJ-Bench-Video [38]. For pairwise preference-based reward models, we randomly permute the order of the two candidates at evaluation time.

4.1.2 Reinforcement Learning for Vision Generation

Text-to-Image Generation. Training. We perform GRPO on FLUX.1-dev [39] using training prompts from UniGenBench++ [40]. Training is conducted on 32 NVIDIA H200 GPUs with 15 sampling steps and 9 rollouts per prompt from the same initial noise, using 3 gradient accumulation steps and a learning rate of 3×10^{-6} . We set $\beta_{KL} = 0$. **Evaluation.** For inference, we use 30 sampling steps and a classifier-free guidance scale of 3.5, following the official configuration. We evaluate in-domain performance on UniGenBench++. For out-of-domain evaluation, we measure semantic consistency on GenEval [41] and T2I-CompBench [42], and assess image quality using UnifiedReward [1], PickScore [15], and the aesthetic predictor [14].

Text-to-Video Generation. Training. We perform GRPO on Wan2.1-T2V-14B [43] using the training prompts provided by [10]. Training is conducted on 32 NVIDIA H200 GPUs with LoRA rank 64 and alpha 128, using 20 sampling steps and 6 rollouts per prompt from the same initial noise. We train with videos at 240×416 resolution with 33 frames, 2 gradient accumulation steps, and a learning rate of 3×10^{-5} . We set $\beta_{KL} = 0.004$.

Evaluation. For inference, we use 30 sampling steps and a classifier-free guidance scale of 5, generating videos at 480×832 resolution with 33 frames, and evaluating the performance on VBench [44].



Figure 3 Qualitative Comparison on Text-to-Image GRPO.

4.2 Results

4.2.1 Reward Model Comparison

We compare our **UNIFIEDREWARD-FLEX** against representative baselines on both image and video preference-evaluation benchmarks. Fixed scorers (e.g., HPSv2 [13], PickScore [15]) and Bradley-Terry preference models (e.g., HPSv3 [17], VideoReward [4]) provide a single global signal that is insensitive to prompt-specific requirements. Besides, UnifiedReward-Think [2] is a strong VLM-as-a-judge baseline that performs multi-modal assessment with long-chain reasoning, but still follows a fixed checklist of evaluation criteria. In contrast, **UNIFIEDREWARD-FLEX** dynamically instantiates fine-grained criteria conditioned on the prompt and visual evidence, yielding more reliable pairwise decisions. **Quantitatively**, as shown in Tab. 1, **UNIFIEDREWARD-FLEX** achieves the best performance across all benchmarks; notably, it improves over UnifiedReward-Think by +3.2 points on MMRB2 and +2.2 points on GenAI-Bench-Video, highlighting the benefit of context-adaptive criterion composition beyond long-chain reasoning alone. **Qualitative** results are provided in Figs. 1 and 2. For example, Fig. 1 highlights our hierarchical, context-adaptive evaluation in a story-implied prompt ("a child healing a wounded kirin"). Starting from common anchor dimensions (semantic alignment, visual quality, and aesthetics), our model instantiates prompt-specific sub-criteria to check core requirements such as subject completeness and style coherence. Crucially, because the prompt implicitly describes a narrative moment rather than a static portrait, the model further augments the evaluation hierarchy with an additional high-level dimension, i.e., "Narrative & Interaction", to judge whether the generation conveys a coherent healing scene with meaningful entity relations. This adaptive criterion composition prevents the evaluation from being dominated by surface-level rendering quality alone, and yields preference judgments that better reflect prompt-critical intent, providing more informative reward supervision for downstream optimization.

Table 4 Quantitative results on VBench. The first seven metrics correspond to the *Quality* type, while the remaining correspond to the *Semantic* type.

Models	Subject Consistency	Background Consistency	Aesthetic Quality	Imaging Quality	Temporal Flickering	Motion Smoothness	Dynamic Degree	Human Action
Wan2.1-T2V-14B w/ VideoReward w/ UnifiedReward-Think	96.6	97.6	62.4	64.9	99.2	98.5	58.6	79.4
	96.7	97.9	62.9	66.5	99.3	98.5	41.6	78.2
	96.4	97.7	63.9	65.2	99.4	98.4	58.3	78.4
w/ UnifiedReward-Flex	96.9	97.8	65.1	66.9	99.3	99.0	70.8	79.9
Models	Color	Spatial Relationship	Scene	Temporal Style	Overall Consistency	Object Class	Multiple Objects	Appearance Style
Wan2.1-T2V-14B	87.7	72.6	28.8	23.6	25.1	79.1	61.8	22.2
w/ VideoReward	87.8	77.0	28.2	23.7	25.3	82.1	70.2	21.0
w/ UnifiedReward-Think	86.1	77.3	27.2	23.8	25.4	78.4	63.0	22.3
w/ UnifiedReward-Flex	89.6	80.8	30.5	24.2	25.6	83.2	70.6	22.4

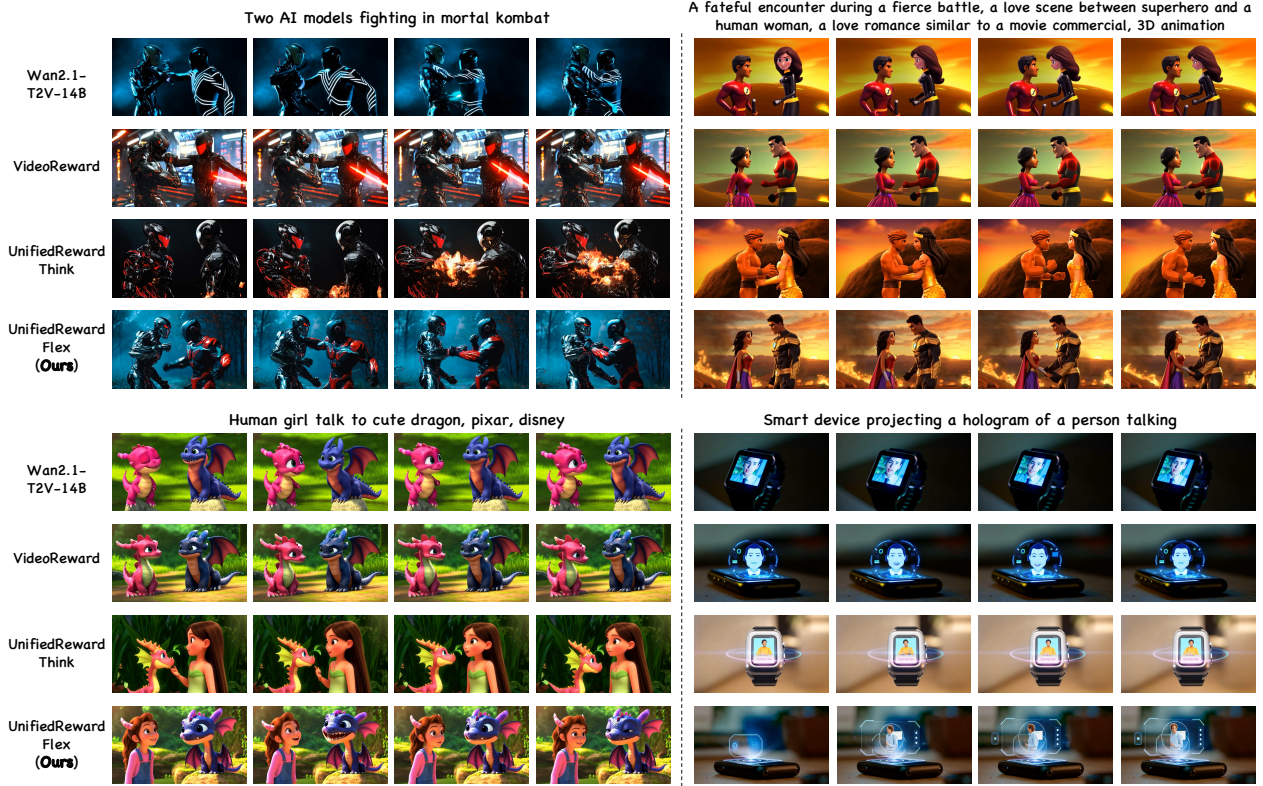


Figure 4 Qualitative Comparison on Text-to-Video GRPO.

4.2.2 Text-to-Image GRPO

Quantitatively, on UniGenBench (Tab. 2), UNIFIEDREWARD-FLEX improves the overall semantic consistency (+14.56) over the base model, and also surpasses the strong VLM-as-a-judge baseline UnifiedReward-Think (+5.06). The improvements are broad-based across challenging dimensions that require compositional and intent-aware evaluation, such as Compound and Logical Reasoning. It also generalizes well to out-of-domain benchmarks (Tab. 3): achieves the best semantic consistency on T2I-CompBench [42] and GenEval [41], while maintaining or improving image quality metrics (e.g., UnifiedReward [1]) compared to other reward baselines. These results indicate that optimizing with our personalized reward does not merely overfit to in-domain prompts; instead, it promotes more robust alignment with diverse prompt intents and visual evidence.

Qualitatively, Fig. 3 further shows that our model better enforces prompt-critical constraints. In the “Newton” example (row 2), the prompt couples multiple requirements (a square falling apple and a circular shadow), which demands reasoning over attributes and geometry. Among the compared methods, only the generator optimized with our reward consistently satisfies this coupled constraint.

Table 5 Hyperparameter Analysis of α . The best results are in **bold**, and the second best are underlined.

Model	Text-to-Image Generation			Model	Text-to-Video Generation		
	UniGenBench	T2I-CompBench	UnifiedReward		Total	Semantic	Quality
FLUX.1-dev	59.39	48.57	3.07	Wan2.1-T2V-14B	80.81	69.66	83.60
$\alpha = 0$ (w/o \bar{R}_{dim})	71.13	50.32	3.25	$\alpha = 0$ (w/o \bar{R}_{dim})	82.46	71.79	85.13
$\alpha = 0.3$	72.50	50.42	3.23	$\alpha = 0.3$	82.56	72.11	85.17
$\alpha = 0.5$	73.10	50.90	3.29	$\alpha = 0.5$	82.82	72.34	85.44
$\alpha = 1$ (w/o R_{overall})	73.44	51.59	3.26	$\alpha = 1$ (w/o R_{overall})	<u>82.89</u>	<u>72.42</u>	<u>85.51</u>
$\alpha = 0.7$ (Ours)	<u>73.95</u>	51.37	3.31	$\alpha = 0.7$ (Ours)	<u>83.08</u>	<u>72.94</u>	<u>85.62</u>



A clever fox opened the treasure chest in front of him because he had solved a complex mystery. The inside of the lid of the box was engraved with the words "Wisdom is the key to all hidden treasures."



An anthropomorphic sculpture of Mr. Moon is watering the stars. The work says "We are all made of stardust and dreams" in a clay style.

Figure 5 Qualitative Results of Text-to-Video Generation during Training Progress.

4.2.3 Text-to-Video GRPO

Quantitatively, Tab. 4 summarizes VBench results for Wan2.1-T2V-14B GRPO with different reward signals. UNIFIEDREWARD-FLEX yields clear improvements on both dynamic quality and compositional semantics. For example, on the *quality* side, it notably boosts the Dynamic Degree score (from 58.6 to 70.8), indicating that our reward provides more informative supervision for motion-intensive generations beyond static appearance. On the *semantic* side, it substantially improves Spatial Relationship (72.6 to 80.8) and Color consistency (87.7 to 89.6), suggesting better prompt grounding in relational and attribute-level constraints. Compared with VideoReward and UnifiedReward-Think, while both baselines also achieve competitive results, their improvements are less pronounced; in particular, they incur drops on Dynamic Degree, indicating limited ability to encourage richer motion. This contrast further supports that our context-personalized evaluation provides more effective reward supervision for GRPO-based video post-training.

Qualitatively, Fig. 4 shows that using UNIFIEDREWARD-FLEX as the reward for GRPO yields more coherent videos under motion- and interaction-centric prompts. In the upper-left example ("Two AI models fighting in Mortal Kombat"), the base Wan2.1-T2V-14B output is largely static, and GRPO with VideoReward or UnifiedReward-Think often further dampens the motion dynamics, resulting in reduced action amplitude and weaker interaction intensity across frames. In contrast, UNIFIEDREWARD-FLEX-guided GRPO preserves stronger, continuous motion and clearer contact-driven progression, better matching the prompt's intent.

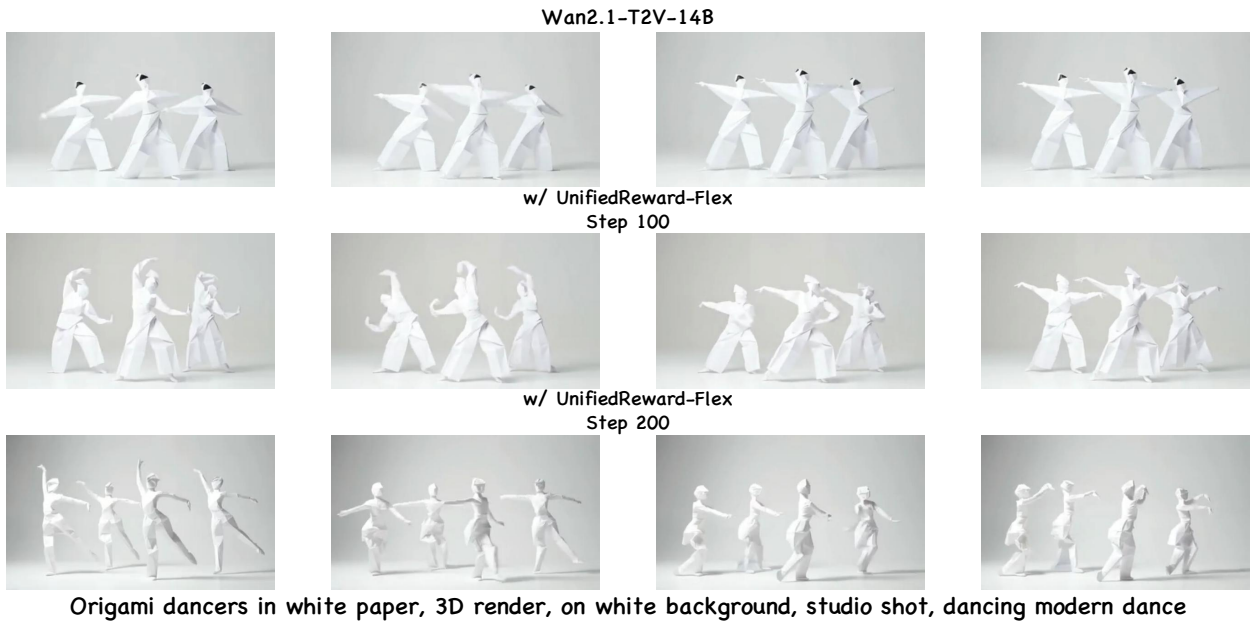


Figure 6 Qualitative Results of Text-to-Video Generation during Training Progress.

Table 6 Comparison of Training Efficiency (Seconds per Step).

	PickScore	HPSv3	UnifiedReward	VideoReward	UnifiedReward-Think	UnifiedReward-Flex
FLUX.1-dev	102s	103s	109s	—	124s	143s
Wan2.1-T2V-14B	—	—	—	285s	328s	336s

4.3 Ablation Studies

Effect of DPO Alignment. As shown in Tab. 1, applying DPO yields consistent improvements, validating the role of preference alignment in sharpening preference discrimination. Importantly, the gains persist even in the “Both correct” setting, where both sampled traces predict the correct final preference. In this harder regime, DPO provides supervision on how the decision is reached: explicitly preferring higher-quality, more context-adaptive reasoning trajectories further improves discriminative accuracy by separating subtle quality differences that are invisible to decision-level correctness alone. Together, these results motivate coupling personalized criterion composition with reasoning-aware preference alignment to build robust reward models for both image and video generation.

Hyperparameter Analysis of α . We analyze the impact of α in Tab. 6, which controls the balance between the averaged dimension-wise win rate (\bar{R}_{dim}) and the overall win rate (R_{overall}) in our reward model. When $\alpha = 0$, the model relies solely on the overall win rate, potentially overlooking finer, context-specific details, resulting in suboptimal performance. As α increases, the model shifts focus towards dimension-wise rewards, capturing more context-adaptive nuances. However, when $\alpha = 1$, the model becomes overly focused on dimension-wise rewards, limiting its ability to assess broader, global preferences. Our results show that $\alpha = 0.7$ strikes an optimal balance, combining context-aware reasoning with global quality assessment, leading to the best performance across both image and video generation tasks. This further demonstrates the effectiveness of our personalized multi-dimensional rewards in enhancing the model’s preference alignment.

4.4 Discussion

Training Efficiency. Tab. 6 compares the per-step training time across different reward models. Fixed scorers and Bradley-Terry-style models (e.g., PickScore, HPSv3) are the most efficient, as they directly output scalar rewards without explicit reasoning. However, this efficiency comes at the cost of coarse and less comprehensive reward signals with limited expressiveness. Reasoning-based VLMs introduce additional overhead. Specifically, UnifiedReward-Think is noticeably slower, since it performs long-chain reasoning under a fixed evaluation rubric to produce judgments. Our UNIFIEDREWARD-FLEX further increases the computation cost, as it goes beyond fixed criteria and conducts context-personalized reasoning: it dynamically

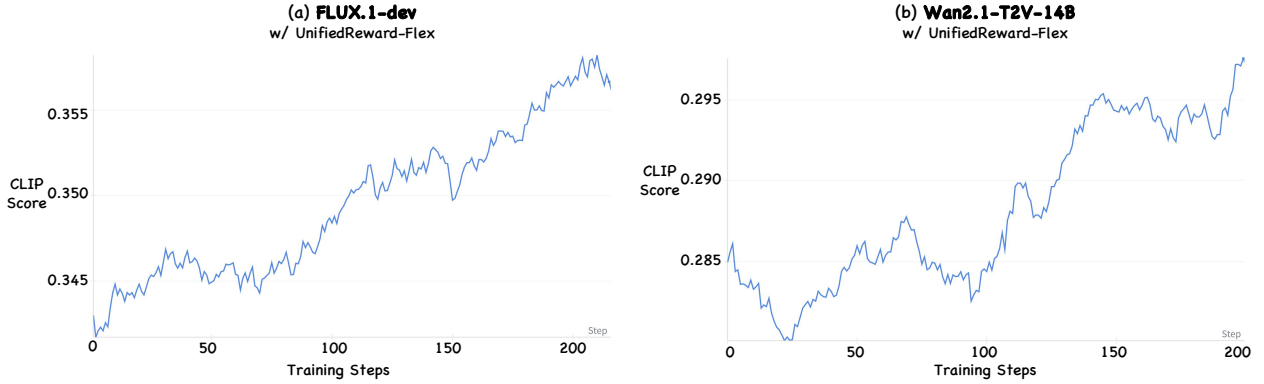


Figure 7 Monitoring Training Progress via CLIP Score.

instantiates fine-grained sub-criteria and, when necessary, introduces new high-level dimensions conditioned on the prompt intent and visual evidence, rather than applying a static checklist. Despite this extra compute, **UNIFIEDREWARD-FLEX** delivers substantially stronger reward accuracy (Tab. 1) and consistently larger gains in GRPO for both image and video generation (Tabs. 3 and 4). These results indicate that the added training cost is a reasonable and practical trade-off for improved alignment quality and generation performance.

Training Progress Visualization. *Quantitatively.* Fig. 7 visualizes the training dynamics when using CLIP score as a proxy metric to monitor semantic alignment during GRPO with **UNIFIEDREWARD-FLEX**. Across both text-to-image (FLUX.1-dev) and text-to-video (Wan2.1-T2V-14B) settings, the CLIP score exhibits a clear and consistent upward trend over training steps, indicating steadily improved prompt-image/video semantic consistency. The similarly stable increase in both domains suggests that our personalized, context-adaptive reward provides reliable optimization signals, reinforcing semantic understanding for both static image synthesis and temporal video generation. *Qualitatively.* Figs. 5 and 6 show a consistent visual improvement trend during GRPO when using **UNIFIEDREWARD-FLEX** as the reward. For image generation (Fig. 5), later checkpoints better enforce prompt-critical constraints and compositional intent (e.g., the chest engraving becomes clearer and more faithful), indicating stronger semantic grounding beyond surface aesthetics. For video generation (Fig. 6), the origami-dancer example evolves from limited, less coordinated motion to smoother, more coherent action progression with improved temporal consistency across frames. Overall, these training-time visualizations corroborate that **UNIFIEDREWARD-FLEX** provides reliable, context-adaptive reward guidance that steadily strengthens both semantic adherence and temporal coherence during training.

5 Conclusion

This paper introduces **UNIFIEDREWARD-FLEX**, a unified personalized reward model that circumvents the limitations of traditional “one-size-fits-all” evaluation in visual generation. By coupling dynamic hierarchical assessment with context-adaptive reasoning, our approach transcends rigid rubrics to capture the nuanced and subjective nature of human preferences. Leveraging a two-stage training pipeline, i.e., structured reasoning distillation and reasoning-aware Direct Preference Optimization (DPO), we demonstrate that **UNIFIEDREWARD-FLEX** yields significantly more precise and context-sensitive reward signals. Empirical validation within the Group Relative Policy Optimization (GRPO) framework reveals that our method consistently outperforms existing baselines, achieving significant improvements in both visual fidelity and semantic alignment for image and video synthesis.

References

- [1] Yibin Wang, Yuhang Zang, Hao Li, Cheng Jin, and Jiaqi Wang. Unified reward model for multimodal understanding and generation. [arXiv preprint arXiv:2503.05236](https://arxiv.org/abs/2503.05236), 2025.
- [2] Yibin Wang, Zhimin Li, Yuhang Zang, Chunyu Wang, Qinglin Lu, Cheng Jin, and Jiaqi Wang. Unified multimodal chain-of-thought reward model through reinforcement fine-tuning. [arXiv preprint arXiv:2505.03318](https://arxiv.org/abs/2505.03318), 2025.
- [3] Yibin Wang, Zhiyu Tan, Junyan Wang, Xiaomeng Yang, Cheng Jin, and Hao Li. Lift: Leveraging human feedback for text-to-video model alignment. [arXiv preprint arXiv:2412.04814](https://arxiv.org/abs/2412.04814), 2024.

[4] Jie Liu, Gongye Liu, Jiajun Liang, Ziyang Yuan, Xiaokun Liu, Mingwu Zheng, Xiele Wu, Qiulin Wang, Wenyu Qin, Menghan Xia, et al. Improving video generation with human feedback. [arXiv preprint arXiv:2501.13918](#), 2025.

[5] Yuhang Zang, Xiaoyi Dong, Pan Zhang, Yuhang Cao, Ziyu Liu, Shengyuan Ding, Shenxi Wu, Yubo Ma, Haodong Duan, Wenwei Zhang, et al. Internlm-xcomposer2.5-reward: A simple yet effective multi-modal reward model. [arXiv preprint arXiv:2501.12368](#), 2025.

[6] Yibin Wang, Zhimin Li, Yuhang Zang, Yujie Zhou, Jiazi Bu, Chunyu Wang, Qinglin Lu, Cheng Jin, and Jiaqi Wang. Pref-grpo: Pairwise preference reward-based grpo for stable text-to-image reinforcement learning. [arXiv preprint arXiv:2508.20751](#), 2025.

[7] Yujie Zhou, Pengyang Ling, Jiazi Bu, Yibin Wang, Yuhang Zang, Jiaqi Wang, Li Niu, and Guangtao Zhai. G2rpo: Granular grpo for precise reward in flow models. [arXiv preprint arXiv:2510.01982](#), 3, 2025.

[8] Jie Wu, Yu Gao, Zilyu Ye, Ming Li, Liang Li, Hanzhong Guo, Jie Liu, Zeyue Xue, Xiaoxia Hou, Wei Liu, et al. Rewarddance: Reward scaling in visual generation. [arXiv preprint arXiv:2509.08826](#), 2025.

[9] Jie Liu, Gongye Liu, Jiajun Liang, Yangguang Li, Jiaheng Liu, Xintao Wang, Pengfei Wan, Di Zhang, and Wanli Ouyang. Flow-grpo: Training flow matching models via online rl. [arXiv preprint arXiv:2505.05470](#), 2025.

[10] Zeyue Xue, Jie Wu, Yu Gao, Fangyuan Kong, Lingting Zhu, Mengzhao Chen, Zhiheng Liu, Wei Liu, Qiushan Guo, Weilin Huang, et al. Dancegrpo: Unleashing grpo on visual generation. [arXiv preprint arXiv:2505.07818](#), 2025.

[11] Junzhe Li, Yutao Cui, Tao Huang, Yinpeng Ma, Chun Fan, Miles Yang, and Zhao Zhong. Mixgrpo: Unlocking flow-based grpo efficiency with mixed ode-sde. [arXiv preprint arXiv:2507.21802](#), 2025.

[12] Alec Radford, Jong Wook Kim, Chris Hallacy, Aditya Ramesh, Gabriel Goh, Sandhini Agarwal, Girish Sastry, Amanda Askell, Pamela Mishkin, Jack Clark, et al. Learning transferable visual models from natural language supervision. In [ICML](#), pages 8748–8763, 2021.

[13] Xiaoshi Wu, Yiming Hao, Keqiang Sun, Yixiong Chen, Feng Zhu, Rui Zhao, and Hongsheng Li. Human preference score v2: A solid benchmark for evaluating human preferences of text-to-image synthesis. [arXiv preprint arXiv:2306.09341](#), 2023.

[14] Chrisoph Schuhmann. Laion aesthetics. <https://github.com/LAION-AI/aesthetic-predictor>, 2022.

[15] Yuval Kirstain, Adam Polyak, Uriel Singer, Shahbuland Matiana, Joe Penna, and Omer Levy. Pick-a-pic: An open dataset of user preferences for text-to-image generation. [NeurIPS](#), 36:36652–36663, 2023.

[16] Ralph Allan Bradley and Milton E Terry. Rank analysis of incomplete block designs: I. the method of paired comparisons. [Biometrika](#), 39(3/4):324–345, 1952.

[17] Yuhang Ma, Xiaoshi Wu, Keqiang Sun, and Hongsheng Li. Hpsv3: Towards wide-spectrum human preference score. In [ICCV](#), pages 15086–15095, 2025.

[18] Xuan He, Dongfu Jiang, Ping Nie, Minghao Liu, Zhengxuan Jiang, Mingyi Su, Wentao Ma, Junru Lin, Chun Ye, Yi Lu, et al. Videoscore2: Think before you score in generative video evaluation. [arXiv preprint arXiv:2509.22799](#), 2025.

[19] Shuai Bai, Keqin Chen, Xuejing Liu, Jialin Wang, Wenbin Ge, Sibo Song, Kai Dang, Peng Wang, Shijie Wang, Jun Tang, et al. Qwen2. 5-vl technical report. [arXiv preprint arXiv:2502.13923](#), 2025.

[20] Bo Li, Yuanhan Zhang, Dong Guo, Renrui Zhang, Feng Li, Hao Zhang, Kaichen Zhang, Peiyuan Zhang, Yanwei Li, Ziwei Liu, et al. Llava-onevision: Easy visual task transfer. [arXiv preprint arXiv:2408.03326](#), 2024.

[21] OpenAI. Update to GPT-5 system card: GPT-5.2. [OpenAI System Card](#), 2025. URL https://cdn.openai.com/pdf/3a4153c8-c748-4b71-8e31-aecbde944f8d/oai_5_2_system-card.pdf.

[22] Qunzhong Wang, Jie Liu, Jiajun Liang, Yilei Jiang, Yuanxing Zhang, Jinyuan Chen, Yaozhi Zheng, Xintao Wang, Pengfei Wan, Xiangyu Yue, et al. Vr-thinker: Boosting video reward models through thinking-with-image reasoning. [arXiv preprint arXiv:2510.10518](#), 2025.

[23] Kevin Clark, Paul Vicol, Kevin Swersky, and David J Fleet. Directly fine-tuning diffusion models on differentiable rewards. [arXiv preprint arXiv:2309.17400](#), 2023.

[24] Mihir Prabhudesai, Russell Mendonca, Zheyang Qin, Katerina Fragkiadaki, and Deepak Pathak. Video diffusion alignment via reward gradients. [arXiv preprint arXiv:2407.08737](#), 2024.

[25] Kimin Lee, Hao Liu, Moonkyung Ryu, Olivia Watkins, Yuqing Du, Craig Boutilier, Pieter Abbeel, Mohammad Ghavamzadeh, and Shixiang Shane Gu. Aligning text-to-image models using human feedback. [arXiv preprint arXiv:2302.12192](#), 2023.

[26] John Schulman, Filip Wolski, Prafulla Dhariwal, Alec Radford, and Oleg Klimov. Proximal policy optimization algorithms. [arXiv preprint arXiv:1707.06347](#), 2017.

[27] Kevin Black, Michael Janner, Yilun Du, Ilya Kostrikov, and Sergey Levine. Training diffusion models with reinforcement learning. [arXiv preprint arXiv:2305.13301](#), 2023.

[28] Ying Fan, Olivia Watkins, Yuqing Du, Hao Liu, Moonkyung Ryu, Craig Boutilier, Pieter Abbeel, Mohammad Ghavamzadeh, Kangwook Lee, and Kimin Lee. Reinforcement learning for fine-tuning text-to-image diffusion models. In [NeurIPS](#), 2023.

[29] Zichen Miao, Jiang Wang, Ze Wang, Zhengyuan Yang, Lijuan Wang, Qiang Qiu, and Zicheng Liu. Training diffusion models towards diverse image generation with reinforcement learning. In [CVPR](#), pages 10844–10853, 2024.

[30] Rafael Rafailov, Archit Sharma, Eric Mitchell, Christopher D Manning, Stefano Ermon, and Chelsea Finn. Direct preference optimization: Your language model is secretly a reward model. [NeurIPS](#), 36:53728–53741, 2023.

[31] Bram Wallace, Meihua Dang, Rafael Rafailov, Linqi Zhou, Aaron Lou, Senthil Purushwalkam, Stefano Ermon, Caiming Xiong, Shafiq Joty, and Nikhil Naik. Diffusion model alignment using direct preference optimization. In [CVPR](#), pages 8228–8238, 2024.

[32] Kai Yang, Jian Tao, Jiafei Lyu, Chunjiang Ge, Jiaxin Chen, Weihan Shen, Xiaolong Zhu, and Xiu Li. Using human feedback to fine-tune diffusion models without any reward model. In [CVPR](#), pages 8941–8951, 2024.

[33] Runtao Liu, Haoyu Wu, Ziqiang Zheng, Chen Wei, Yingqing He, Renjie Pi, and Qifeng Chen. Videodpo: Omni-preference alignment for video diffusion generation. In [CVPR](#), pages 8009–8019, 2025.

[34] Daya Guo, Dejian Yang, Haowei Zhang, Junxiao Song, Ruoyu Zhang, Runxin Xu, Qihao Zhu, Shirong Ma, Peiyi Wang, Xiao Bi, et al. Deepseek-r1: Incentivizing reasoning capability in llms via reinforcement learning. [arXiv preprint arXiv:2501.12948](#), 2025.

[35] Haoyou Deng, Keyu Yan, Chaojie Mao, Xiang Wang, Yu Liu, Changxin Gao, and Nong Sang. Densegrpo: From sparse to dense reward for flow matching model alignment. [arXiv preprint arXiv:2601.20218](#), 2026.

[36] Dongfu Jiang, Max Ku, Tianle Li, Yuansheng Ni, Shizhuo Sun, Rongqi Fan, and Wenhui Chen. Genai arena: An open evaluation platform for generative models. [arXiv preprint arXiv:2406.04485](#), 2024.

[37] Yushi Hu, Reyhane Askari-Hemmat, Melissa Hall, Emily Dinan, Luke Zettlemoyer, and Marjan Ghazvininejad. Multimodal rewardbench 2: Evaluating omni reward models for interleaved text and image. [arXiv preprint arXiv:2512.16899](#), 2025.

[38] Haibo Tong, Zhaoyang Wang, Zhaorun Chen, Haonian Ji, Shi Qiu, Siwei Han, Kexin Geng, Zhongkai Xue, Yiyang Zhou, Peng Xia, Mingyu Ding, Rafael Rafailov, Chelsea Finn, and Huaxiu Yao. Mj-video: Fine-grained benchmarking and rewarding video preferences in video generation, 2025. URL <https://arxiv.org/abs/2502.01719>.

[39] Black Forest Labs. Flux. <https://github.com/black-forest-labs/flux>, 2024.

[40] Yibin Wang, Zhimin Li, Yuhang Zang, Jiazi Bu, Yujie Zhou, Yi Xin, Junjun He, Chunyu Wang, Qinglin Lu, Cheng Jin, et al. Unigenbench++: A unified semantic evaluation benchmark for text-to-image generation. [arXiv preprint arXiv:2510.18701](#), 2025.

[41] Dhruba Ghosh, Hannaneh Hajishirzi, and Ludwig Schmidt. Geneval: An object-focused framework for evaluating text-to-image alignment. [NeurIPS](#), 36:52132–52152, 2023.

[42] Kaiyi Huang, Kaiyue Sun, Enze Xie, Zhenguo Li, and Xihui Liu. T2i-compbench: A comprehensive benchmark for open-world compositional text-to-image generation. [NeurIPS](#), 36:78723–78747, 2023.

[43] Team Wan et al. Wan: Open and advanced large-scale video generative models. [arXiv preprint arXiv:2503.20314](#), 2025.

[44] Ziqi Huang, Yinan He, Jiashuo Yu, Fan Zhang, Chenyang Si, Yuming Jiang, Yuanhan Zhang, Tianxing Wu, Qingyang Jin, Nattapol Chanpaisit, Yaohui Wang, Xinyuan Chen, Limin Wang, Dahua Lin, Yu Qiao, and Ziwei Liu. VBench: Comprehensive benchmark suite for video generative models. In [Proceedings of the IEEE/CVF Conference on Computer Vision and Pattern Recognition](#), 2024.

Appendix



Figure 8 More Qualitative Result of UNIFIEDREWARD-FLEX on Image Generation Personalized Reward Reasoning.



Figure 9 More Qualitative Result of UNIFIEDREWARD-FLEX on Video Generation Personalized Reward Reasoning.